Hindawi
Mathematical Problems in Engineering
Volume 2021, Article ID 6673816, 12 pages
https://doi.org/10.1155/2021/6673816

Research Article

Comfort Evaluation of Double-Sided Catwalk for Suspension Bridge due to Wind-Induced Vibration

Zhi-Guo Li,[1,2] **Fan Chen**,[3] **Cheng Pei**,[2] **Jia-Ming Zhang**,[2] **and Xin Chen**[2]

[1]*School of Civil Engineering, Southwest Jiaotong University, Chengdu 610031, China*
[2]*Key Laboratory for Wind Engineering of Sichuan Province, Chengdu 610031, China*
[3]*Power-China Road-Bridge Group Co. LTM, Beijing, China*

Correspondence should be addressed to Zhi-Guo Li; lizhiguo@swjtu.edu.cn

Received 29 October 2020; Revised 17 February 2021; Accepted 23 February 2021; Published 11 March 2021

Academic Editor: Giovanni Lancioni

Buffeting response of a double-sided catwalk designed for Maputo Bridge was investigated considering wind load nonlinearity, geometric nonlinearity, and self-excited forces. Buffeting analysis was conducted in time domain using an APDL-developed program in ANSYS, and the results were compared with the buffeting response under the traditional linear method. The wind field was simulated using the spectra representation method. Aerostatic coefficients were obtained from section model wind tunnel test. Parameter study has been carried out to investigate the effects of cross bridge interval and the gantry rope diameter on buffeting response. Referring to the ISO 2631-1(1997) standard and the annoyance rate model, the comfort of catwalk due to wind-induced vibration was evaluated. The results indicate that traditional linear calculation methods will underestimate the buffeting response of the catwalk, and enlarging the gantry rope size as well as decreasing the cross bridge interval would increase the comfort level. Moreover, the effect of gantry rope diameter was obvious than that of cross bridge interval. Annoyance rate model can evaluate the comfort level quantitatively compared to the ISO standard.

1. Introduction

Catwalk structures are temporary walkways used in the erection of main cables in suspension bridges, consisting of a few ropes, steel cross beams, wooden steps, and porous wire meshes at the bottom and both sides [1]. When the catwalk is not fixed on the main cables, the catwalk system is more vulnerable to the wind-induced vibration. Experts designed a catwalk for the Akashi Kaikyo Bridge, including traction system, erection method, static deformation, static wind stability, lateral passage setting, and vibration control measures [2–4]. A catwalk model with a reduction ratio of 1/14 and 1/4 was used to study the influence of the Reynolds number and windshield rate on the aerostatic coefficients through wind tunnel tests. At the same time, the effect of the number of cross bridge on dynamic response was studied through buffeting analysis [5]. To ensure the safety of the main cable in cross wind during construction, some studies focus on the influence of catwalk design parameters on the galloping of main cables [6, 7].

Due to turbulence in natural wind, the catwalk will vibrate randomly. If the wind speed is high enough, the vibration causes adverse effects for those who work on the site. The psychology of construction workers will be affected by catwalk vibration, including electromyogram (EMG), organ dysfunction, and phenomenon of subjective perception declination. Meanwhile, their irritability and error rate would increase, resulting in fatigue easily, thereby reducing the efficiency of construction and affecting the quality of main cable erection. Therefore, it is necessary to evaluate the comfort level of catwalk due to wind induced vibration. Researchers put their focus on the aerostatic stability and buffeting response of catwalks. The influence of yaw angle and turbulent wind were considered to analyze the stability of catwalk by using the nonlinear finite element method [8]. The mechanism of unique coupling between vertical and lateral vibrations of catwalk was discussed in the buffeting analysis [9]. The influence of cross bridge interval was evaluated only for catwalk's buffeting response.

In terms of comfort evaluation, a lot of researches have been done based on the vibration of vehicles, high-rise buildings, offshore platforms, etc. [10–12]. However, few researches about the comfort evaluation of temporary structures, like catwalk, have been reported. Comfort evaluation for those structures always focuses on the level of human subjective feelings to the vibration based on traditional methods. However, the level of subjective feelings is influenced by many factors, including the psychological and physiological ones. So the traditional methods can hardly evaluate the comfort level quantitatively. Therefore, the introduction of annoyance rate model is an appropriate supplement. An appropriate annoyance rate model will improve the accuracy of the research.

Taking the double-sided catwalk of a highway suspension bridge as an example, section model wind tunnel test was conducted to get aerostatic coefficients of the catwalk section, as shown in Figure 1. In the following section, the fluctuating wind field was simulated by the spectral representation method. With these parameters, nonlinearity of wind load was considered in buffeting response analysis, as well as geometric nonlinearity of catwalk in Section 3. Based on the buffeting response, this study evaluates its comfort due to wind-induced vibration according to the ISO 2631-1-1997 standard and annoyance rate model in Section 4. Results show both enlarging the gantry rope size and decreasing the cross bridge interval would boost the comfort level. But change of the cross bridge interval plays a less significant role. What is more, annoyance rate model can evaluate the comfort level quantitatively compared to the ISO standard.

2. Wind Tunnel Test

The catwalk is designed for Maputo highway suspension bridge, which belongs to the "Maputo Bridge and Link Roads Project." It will become the longest suspension bridge in Africa, in the bay of Maputo, with a main span of 680 m and sag ratio of 1/10. The span configuration is 260 m (Maputo side) + 680 m (midspan) + 491 m (north span) for the main cable. The catwalk rope is parallel to the main cable with a separation distance of 1.5 m. There are 11 cross bridges distributed every 120 m along the span, with 1 in each side span and 5 in midspan. Gantries are distributed every 40 m or 50 m along the span. The left side and right side of the catwalk have a distance of 42 m. Each side of the catwalk is 4.2 m in width. The catwalk rope is size of φ 54 type and gantry rope is the size of φ 60. Detailed design of the catwalk section is shown in Figure 2.

An industrial wind tunnel (XNJD-1) was used at Southwest Jiaotong University for the investigation of the static wind loading, lift, drag, and moment. The test section was equipped with a rig and force balance system for the static wind loading testing of the bridge section. To investigate the aerodynamic performance of catwalk at large angle of attack, as Figure 3 shows, a 1 : 10 scale model is tested in the XNJD-1 wind tunnel under smooth flow to get the tricomponent static aerodynamic coefficients, with the angle of attack varying from −20° to 20° every degree each, and

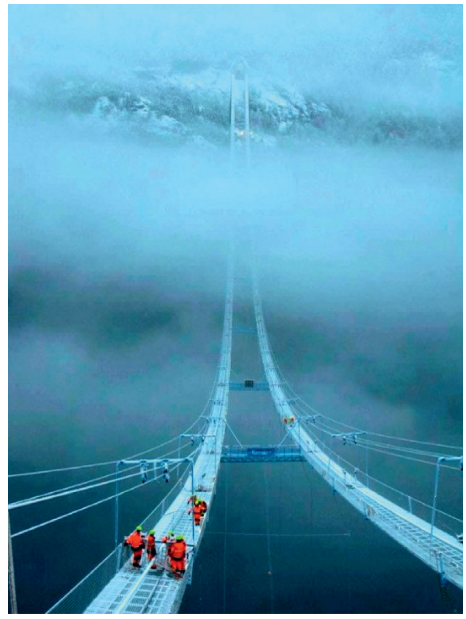

Figure 1: Double-sided catwalk schematic diagram.

three wind speeds were set (10 m/s, 15 m/s, and 20 m/s). Details about the test section in XNJD-1 wind tunnel can be found in [13]. The section model of catwalk is 2.1 m long, 0.84 m wide, and 0.29 m high, of which is made up of steel, meshwork, and wood. Drag force, lift force, and pitching moment force coefficients are derived from equations (1)–(3) and shown in Figure 4. The testing results from different wind speeds are identical, thus indicating that the influence of Reynolds number could be neglected.

$$C_D(\alpha) = \frac{F_D(\alpha)}{(1/2)\rho V^2 HL}, \tag{1}$$

$$C_L(\alpha) = \frac{F_L(\alpha)}{(1/2)\rho V^2 BL}, \tag{2}$$

$$C_M(\alpha) = \frac{M_z(\alpha)}{(1/2)\rho V^2 B^2 L}, \tag{3}$$

where $C_D(\alpha)$, $C_L(\alpha)$, and $C_M(\alpha)$ are the drag force, lift force, and pitching moment force coefficients, respectively, F_D, F_L, and M_z are the measured drag force, lift force, and pitching moment, respectively, α is the angle of attack, ρ is the air density, V is the wind velocity, and H, B, and L are the height, width, and length of the catwalk model, respectively.

3. Time Domain Buffeting Analysis for the Catwalk

3.1. Finite Element Model. Catwalk is the typical cable-truss structure, which is stabilized by the initial tension in the ropes. With the loads acting on the catwalk, the deformation including the rigid body displacement and strain develops, thus changing the structure stiffness. So the influence of large deformation and prestress should be considered in the finite element model. Ansys 15.0 is software adopted here to

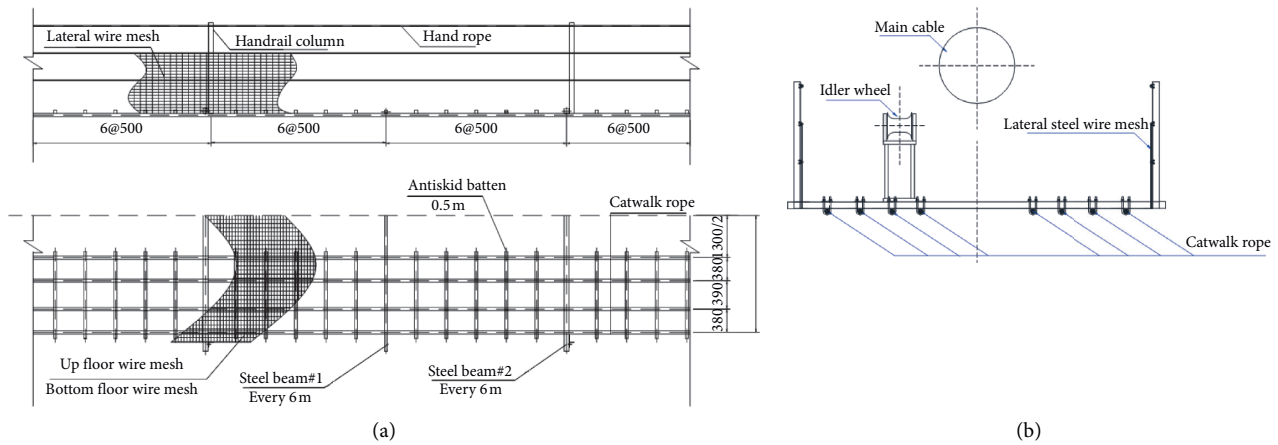

Figure 2: Detailed design of the catwalk section. (a) Elevation view and vertical view. (b) Lateral view.

Figure 3: Catwalk section model of Maputo Bridge tested in wind tunnel.

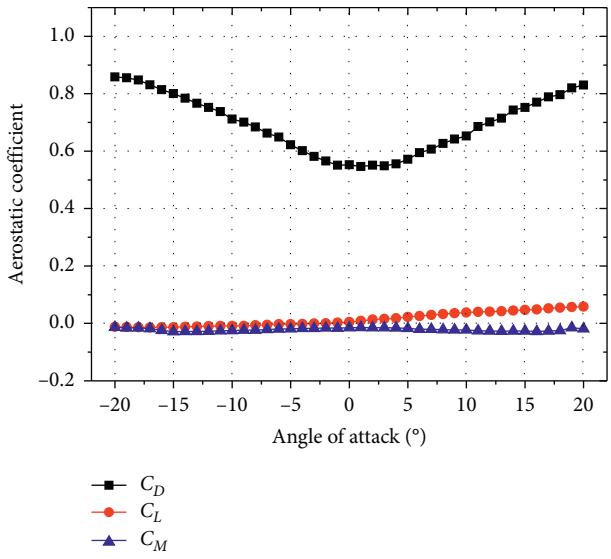

Figure 4: Aerostatic coefficients of catwalk for Maputo Bridge.

develop the finite element model. The catwalk load-bearing ropes are only under tension, use link 10 units, and use the keyopt command to eliminate the stiffness matrix of the load-bearing rope units so that they can only withstand the tension. Catwalk beams, door frames, and other structures can withstand tension, pressure, and bending moments, so use beam 44 unit for simulation. For catwalk handrails, wire mesh, hand ropes, and other components, calculate the total mass and then divide by the number of load-bearing ropes to get the average weight of each load-bearing rope. When defining the characteristics of the load-bearing rope, increase the density of the load-bearing rope based on the calculated average mass. Cross bridges are modeled by an equivalent beam with the same mass and stiffness properties. Handrail column, hand rope, and meshwork network have less contribution to the whole stiffness of the catwalk, so they are represented by some equally distributed mass on the finite element model. Janssen et al. [11] found that bridge tower had little influence on the dynamic properties of the catwalk, so the bridge tower is neglected in the finite element model. Nodes on the tower top and ends of the catwalk are constrained all degrees of freedom. The three-dimensional finite element model is shown in Figure 5.

With the finite element above, its modal analysis was conducted and the first 10 modes are listed in Table 1. And the first lateral bending, vertical bending, and torsion modal shape are shown in Figures 6 ~ 8.

3.2. Simulation of Wind Field. The fluctuating wind velocity field was simulated by the spectral representation method with the Cholesky explicit decomposition [14] of cross-spectral density matrix. It is assumed that fluctuating wind field characteristics change along the direction of span but also change along the direction of height. It is usually assumed that the wind fluctuations in three orthogonal directions are mutually uncorrelated. The overall 3D (i.e., three components of natural wind) wind velocity field can be simplified into many one-dimensional wind velocity fields. Deodatis [15] adopted the FFT (fast Fourier transform) technique, and the computational efficiency was further improved. Then random field in terms of lateral and vertical components was generated at 100 locations along the span of the catwalk with a separation of around 18 meters. The other details for simulating the wind field are listed in Table 2. The wind velocity of the middle node in the midspan is chosen to verify the simulated time series. The velocity pieces are shown in Figure 9.

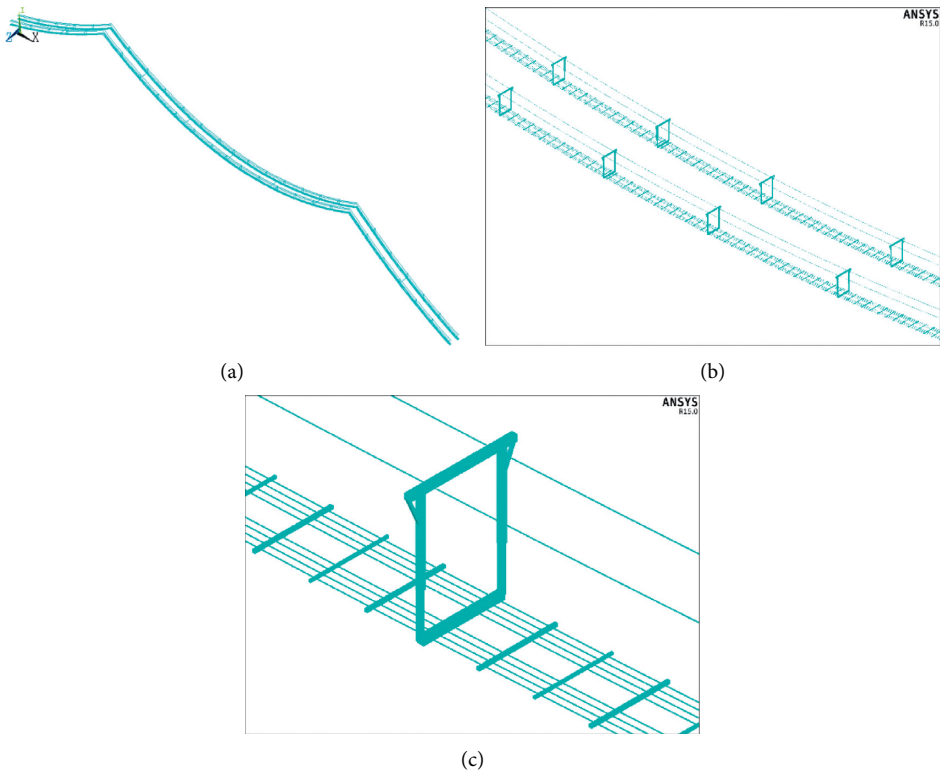

Figure 5: The three-dimensional finite element model. (a) Full finite element model of catwalk for Maputo Bridge. (b) Local finite element model. (c) Local finite element model.

Table 1: Modal frequencies and shapes.

Mode number	Characteristics of modal shapes	Modal frequency (Hz)
1	1st symmetric lateral bending	0.06629
2	1st antisymmetric vertical bending	0.12705
3	1st antisymmetric vertical bending + 1st antisymmetric torsion	0.13171
4	1st antisymmetric vertical bending + 1st symmetric torsion	0.13435
5	1st right span antisymmetric vertical bending	0.16159
6	1st symmetric vertical bending	0.18639
7	1st lateral bending of left side span	0.18682
8	1st antisymmetric torsion	0.19459
9	1st symmetric torsion	0.19763
10	2nd antisymmetric torsion	0.21966

When the time series of wind velocity is simulated, the power spectra density can be calculated using the FFT. As Figure 10 shows, the simulation spectrum fits the target spectrum well, indicating the correctness of the simulation.

3.3. Finite Element Model. The buffeting force caused by fluctuating wind is usually expressed in the quasisteady form. Aerodynamic admittance is introduced to correct the quasisteady formulae. So the buffeting forces acting on the catwalk are given as follows:

$$L_b(t) = \frac{1}{2}\rho U^2 B\left(2C_L\chi_{Lu}\frac{u(t)}{U} + (C_L' + C_D)\chi_{Lw}\frac{w(t)}{U}\right), \quad (4)$$

$$D_b(t) = \frac{1}{2}\rho U^2 B\left(2C_D\chi_{Du}\frac{u(t)}{U} + (C_D' - C_L)\chi_{Dw}\frac{w(t)}{U}\right), \quad (5)$$

$$M_b(t) = \frac{1}{2}\rho U^2 B^2\left(2C_M\chi_{Mu}\frac{u(t)}{U} + C_M'\chi_{Mw}\frac{w(t)}{U}\right), \quad (6)$$

where χ_{Lu}, χ_{Lw}, χ_{Du}, χ_{Dw}, χ_{Mu}, and χ_{Mw} are aerodynamic admittance function, reflecting the connection between fluctuating wind and buffeting force. For simplicity, aerodynamic admittance function is set as constant 1. The buffeting analysis was conducted at 0 attack angle, and the related aerodynamic static coefficients and derivatives are $C_L = 0.0051$, $C_D = 0.5526$, $C_M = -0.0150$, $C_D' = 0.0905$, $C_L' = 0.1295$, and $C_M' = 0.1037$.

3.4. Self-Excited Force in FE Analysis. Based on the flutter theory proposed in [16], the self-excited force can be expressed using 18 flutter derivatives as follows:

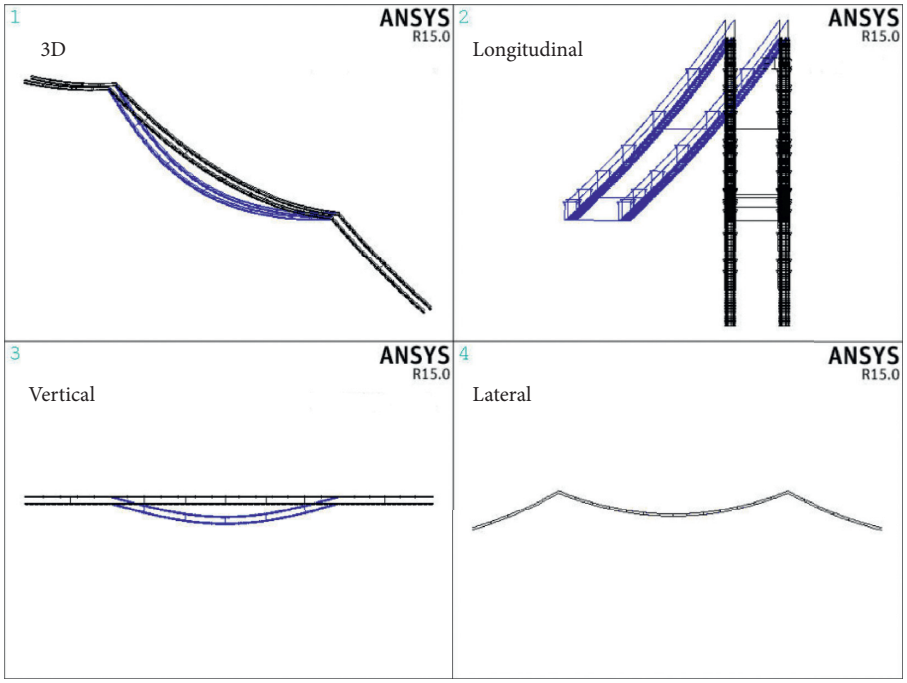

Figure 6: First lateral bending mode.

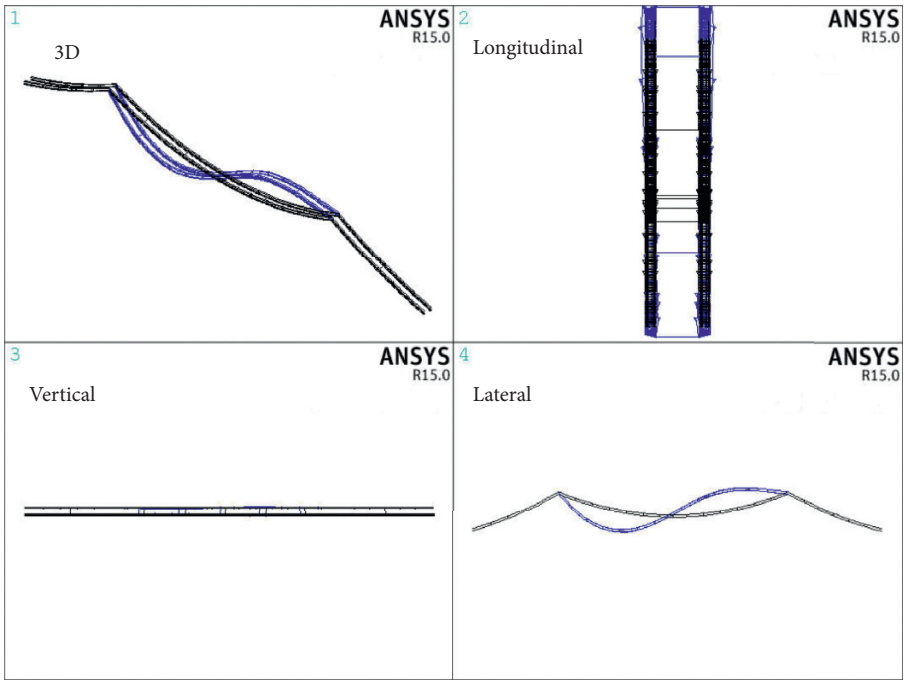

Figure 7: First vertical bending mode.

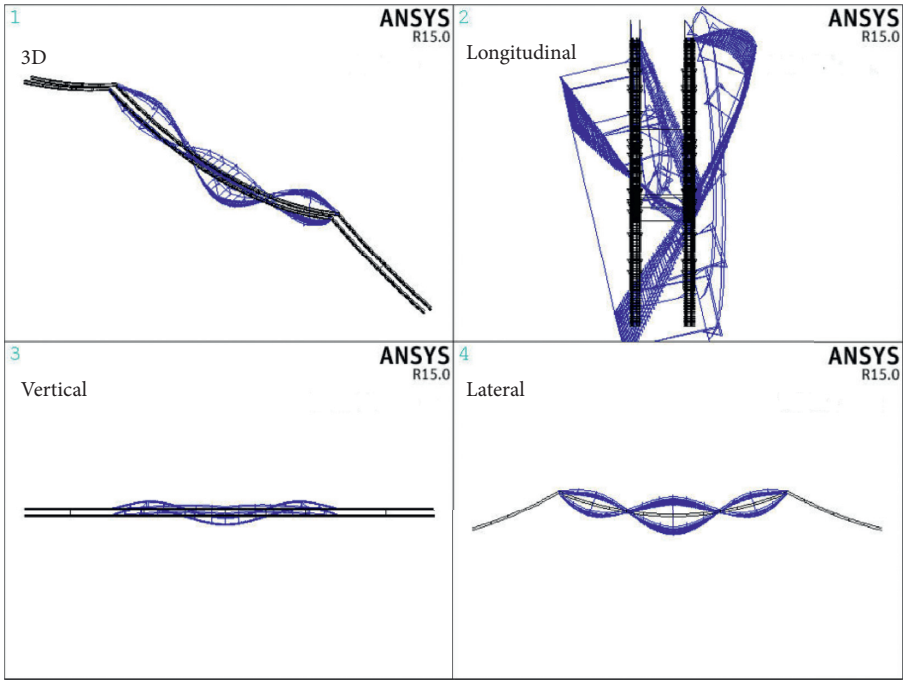

Figure 8: First torsion mode.

Table 2: Parameters for simulating the wind field.

Number of simulated nodes	100
V_{10}	15 m/s
Separation of frequency	1024
Upper limit of frequency	2 Hz
Lower limit of frequency	0.1 Hz
Longitudinal wind spectra	Simiu spectra
Vertical wind spectra	Lumley–Panofsky spectra
Ground roughness length z0	0.03 m
Decaying factor Cz	10
Decaying factor Cy	16
Decaying factor Cw	8
Time interval	0.25 s

Note: $V_{10} = 15$ m/s is considered as the maximum wind speed for construction according to engineering practice.

$$L_{se} = \frac{1}{2}\rho U^2 (2B)\left(KH_1^*\frac{\dot{h}}{U} + KH_2^*\frac{B\dot{\alpha}}{U} + K^2H_3^*\alpha + K^2H_4^*\frac{h}{B} + KH_5^*\frac{\dot{p}}{U} + K^2H_6^*\frac{p}{B}\right),$$

$$D_{se} = \frac{1}{2}\rho U^2 (2B)\left(KP_1^*\frac{\dot{p}}{U} + KP_2^*\frac{B\dot{\alpha}}{U} + K^2P_3^*\alpha + K^2P_4^*\frac{p}{B} + KP_5^*\frac{\dot{h}}{U} + K^2P_6^*\frac{h}{B}\right), \tag{7}$$

$$M_{se} = \frac{1}{2}\rho U^2 \left(2B^2\right)\left(KA_1^*\frac{\dot{h}}{U} + KA_2^*\frac{B\dot{\alpha}}{U} + K^2A_3^*\alpha + K^2A_4^*\frac{h}{B} + KA_5^*\frac{\dot{p}}{U} + K^2A_6^*\frac{p}{B}\right),$$

where ρ is the air density, U is mean wind velocity, B is the width of the catwalk, $K = (B\omega/U)$ is reduced frequency, and H_i^*, P_i^*, A_i^* $(i = 1, 2, \ldots, 6)$ are the flutter derivatives.

L_{se}, D_{se}, and M_{se} stand for the self-excited lift, drag, and pitching moment, and their direction and relation with B and α are shown in Figure 11.

To facilitate the calculation in the finite element software ANSYS, the self-excited force can be rewritten in the following matrix form:

$$\left[F_{se}^i\right] = \left[C_{se}^i\right]\left\{\dot{X}\right\} + \left[K_{se}^i\right]\{X\}, \tag{8}$$

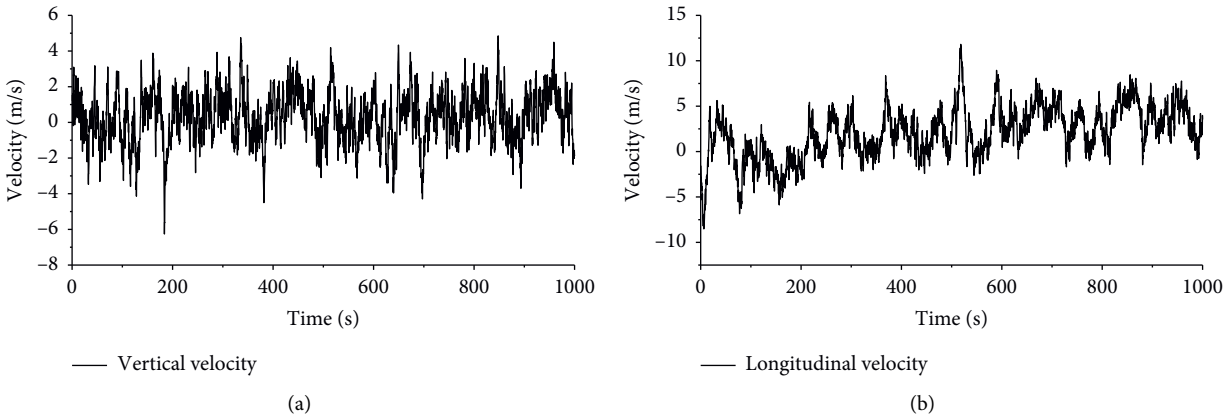

Figure 9: Simulated wind velocity of the middle node in the midspan. (a) Part of the vertical wind velocity series. (b) Part of the longitudinal wind velocity series.

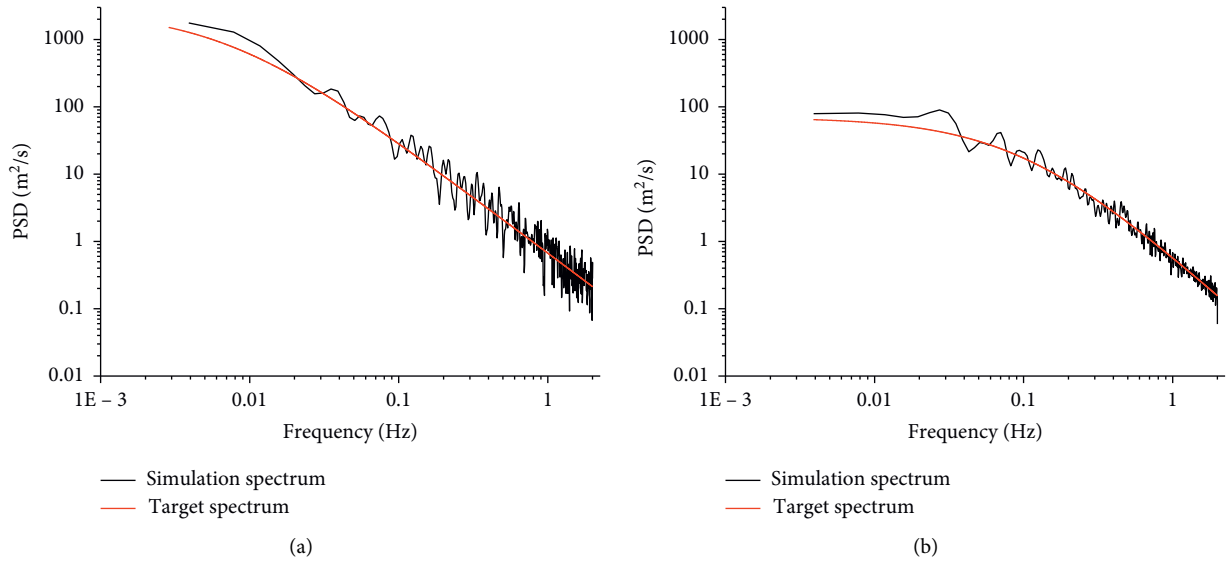

Figure 10: Comparison of simulation PSD and target PSD. (a) Longitudinal wind velocity PSD. (b) Vertical wind velocity PSD.

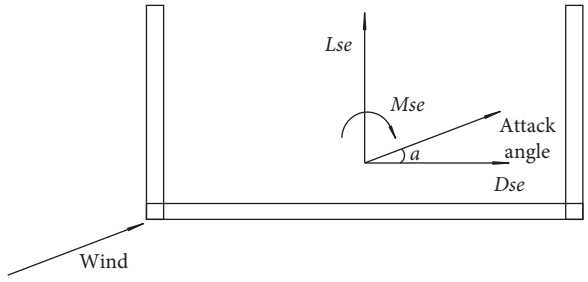

Figure 11: Self-excited forces on catwalk section.

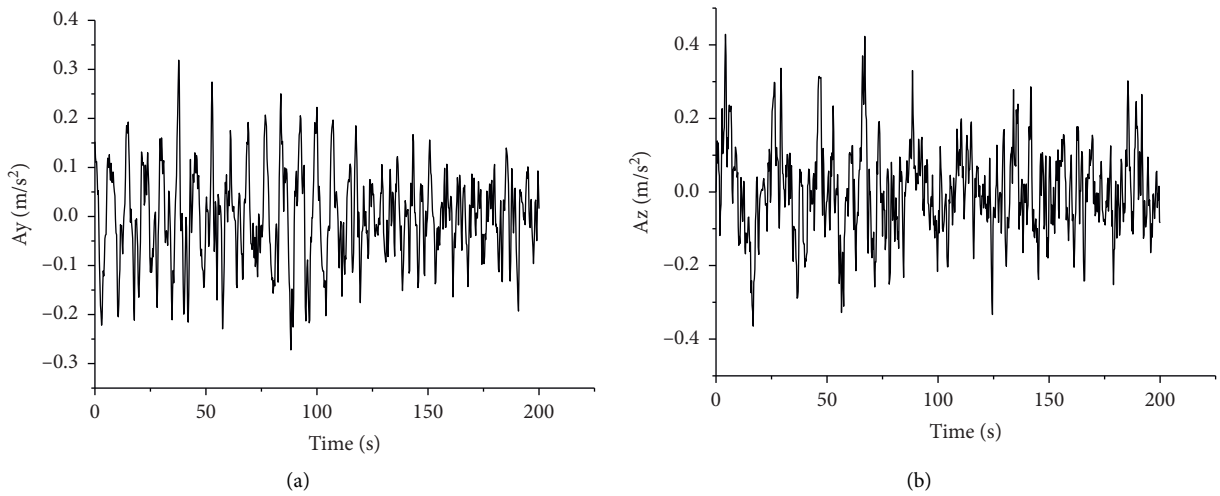

Figure 12: Time history of acceleration response of the middle node in the midspan. (a) Vertical acceleration time history. (b) Lateral acceleration time history.

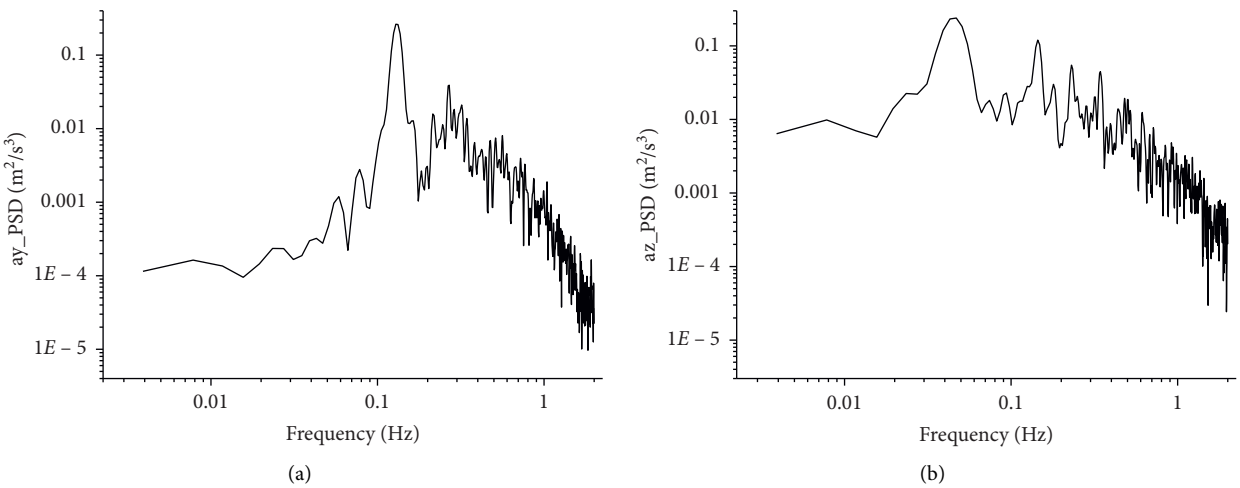

Figure 13: PSD of acceleration response of the middle node in the midspan. (a) Vertical acceleration PSD. (b) Lateral acceleration PSD.

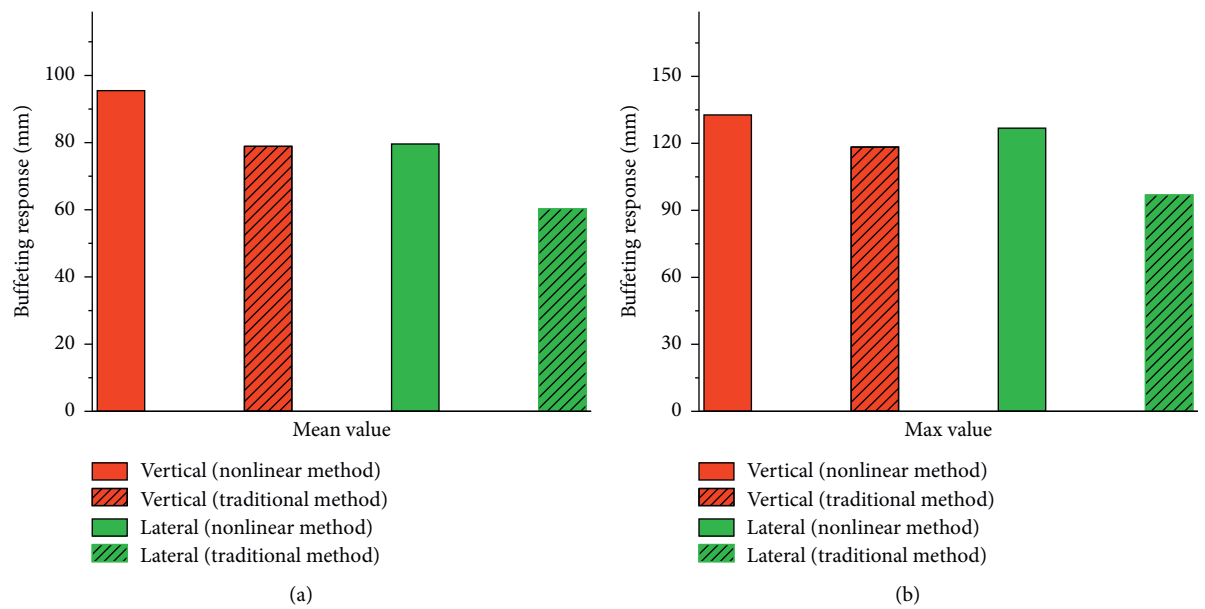

Figure 14: RMS of buffeting response of the middle node in the midspan. (a) Mean value. (b) Max value.

where $[C_{se}^i]$ and $[K_{se}^i]$ are the aerodynamic damping and stiffness matrix, respectively. In that case, self-exited force is realized using the Matrix 27 element in ANSYS, which has 12 degrees of freedom, to represent the aerodynamic damping and stiffness.

To facilitate the calculation, flutter derivatives are derived from the closed form suggested by Simiu and Scanlan [15]:

$$\begin{aligned}
H_1^* &= -\frac{C_L'}{2K}, \\
H_2^* &\approx -\frac{C_L'}{2K} n_x, \\
H_3^* &\approx -\frac{C_L'}{2K^2}, \\
H_4^* &= 0, \\
A_1^* &= \frac{C_M'}{2K}, \\
A_2^* &= -\frac{C_M'}{2K^{n_\theta}}, \\
A_3^* &\approx \frac{C_M'}{2K^2}, \\
A_4^* &= 0, \\
n_x(K) &= \frac{A_1^*}{H_1^*}, \\
n_\theta(K) &= \frac{A_3^*}{H_3^*}, \\
P_1^* &= -\frac{1}{K} C_D, \\
P_2^* &= \frac{1}{2K} C_D', \\
P_3^* &= \frac{1}{2_K^2} C_D', \\
P_5^* &= \frac{1}{2K} C_D', \\
H_5^* &= \frac{1}{K} C_L, \\
A_5^* &= -\frac{1}{K} C_M, \\
P_4^* &= P_6^* = H_6^* = A_6^* = 0,
\end{aligned} \tag{9}$$

where C_L' and C_M' are the derivatives of lift coefficients and pitching moment coefficients considering attack angle, K is the reduced frequency, and n_x and n_θ are transforming factors for vertical motion and torsional motion, respectively.

3.5. Buffeting Response of Catwalk. By conducting the time domain analysis, we can get the buffeting responses of the catwalk. The lateral and vertical acceleration responses of the middle node in the midspan are shown in Figure 10. Their power spectra density is shown in Figure 12. The power spectra density of acceleration response of the middle node in the midspan is shown in Figure 13. The response frequency is close to the 1st lateral and vertical bending modal frequency, thus indicating the accuracy of the time domain buffeting analysis. At the same time, Figure 14 shows the comparison RMS results of the buffeting response of the nonlinear method and the traditional linear method. The results show that the traditional linear method will underestimate the buffeting response of the catwalk, and the maximum error exceeds 16.7%.

4. Comfort Evaluation of Catwalk

4.1. Comfort Evaluation Based on ISO 2631 Standard. According to the buffeting analysis results in the previous section, the catwalk vibrates in a frequency range less than 0.5 Hz. So vibration of the catwalk is evaluated based on the part of ISO 2631-1-1997 for evaluating the incidence of motion of sickness (apply to motion frequencies below 0.5 Hz) [17]. Referring to the standard, the weighted root mean square (RMS) of the acceleration shall be determined first. Although the vibration shall be assessed only with respect to the overall weighted acceleration in the z-axis, using this method to evaluate the vibration of the catwalk in the y-axis can also indicate the comfort level qualitatively to some extent. The weighted RMS acceleration value is given by

$$A_{rms} = \left[\frac{1}{T} \int_0^T a_w^2(t) \mathrm{d}t \right]^{(1/2)}, \tag{10}$$

where a_w is the frequency weighted acceleration and T is the lasting time of vibration.

This standard recommends a single frequency weighting Wf for the evaluation of the effects of vibration on the incidence of motion sickness. In this study, it is assumed the time fluctuating wind acting on the catwalk is the same, so the vibration time is neglected in the evaluation. When the weighted RMS acceleration is calculated, the comfort level can be determined referring to Table 3. The frequency weighting curves for principal weighting are shown in Figure 15.

4.2. Comfort Evaluation Based on Annoyance Rate Model. Compared to ISO 2631-1-1997, this method based on annoyance rate model can further estimate quantitatively the number of constructors on site who feel discomfort due to vibration. A fuzzily random evaluation model on the basis of annoyance rate for human body's subjective response to vibration, with relevant fuzzy membership function and probability distribution given, is presented. When assessing the

Table 3: Reactions to several magnitudes of overall vibration.

Frequency weighted RMS acceleration aw ($m \cdot s^{-2}$)	Subjective response
$a_w < 0.315$	Not uncomfortable
$0.315 \le a_w < 0.63$	A little uncomfortable
$0.5 < a_w < 1$	Fairly uncomfortable
$0.8 < a_w < 1.6$	Uncomfortable
$1.25 < a_w < 2.5$	Very uncomfortable
$a_w > 2$	Extremely uncomfortable

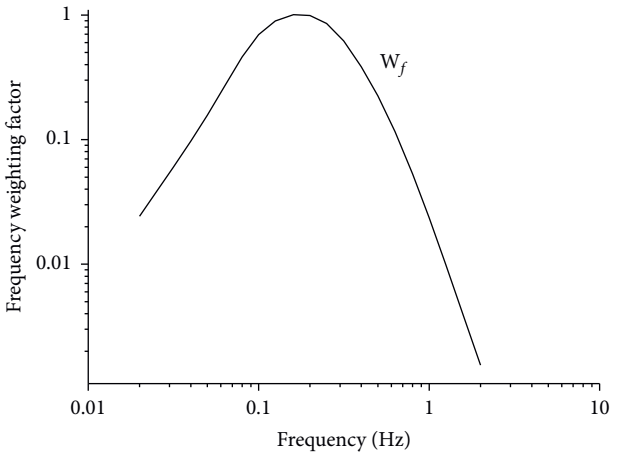

Figure 15: Frequency weighting curves for principal weighting.

vibration comfort, many different psychophysical and physical factors, such as individual susceptibility, body characteristics, and posture together with the frequency, direction, magnitude, and duration of vibration, are relevant in development of unwanted effects [18]. The annoyance threshold acceleration determined by the two-valued logic method cannot describe the ambiguity and randomness existing in human response to vibration environments, which results in many uncertainties in the vibration comfort based reliability analysis. All these uncertainties were analyzed from a view point of psychophysics. The membership function and corresponding conditional probability distribution were determined based on the format of field survey table and laboratory findings.

A fuzzy stochastic model for human response to vibrations was presented. Song [19] combined the fuzzy logic method, the probability theory, and the experimental statistics, to advance a new evaluation index, i.e., annoyance rate method.

Annoyance rate is the rate of unacceptable response under certain vibration intensity. The vibration sensitivity is different according to different range of frequency. The root mean square (vibration intensity) of weighted frequency is adopted internationally as the foundation for evaluating the vibration comfort. The vertical general frequency weighted function can be expressed as follows:

$$W_{fj} = \begin{cases} 0.5 f^{-.5}, & 0 \le f \le 4, \\ 1, & 4 \le f \le 8, \\ 8 f^{-1}, & 8 \le f \le 80, \end{cases} \tag{11}$$

and the vibration intensity a_w is given by

$$a_w = W_{fj} a_{rms}, \tag{12}$$

where a_{rms} is the RMS acceleration value. Annoyance rate indicates the ratio of people who cannot accept the external stimulus to the total statistical people. It can be used to determine the annoyance threshold for vibration comfort. Annoyance threshold means the limit of acceleration on the premise of ensuring acceptable comfort. Under discrete distribution, the annoyance rate can be expressed as follows:

$$A(a_{wi}) = \frac{\sum_{j=1}^{m} v_j n_{ij}}{\sum_{j=1}^{m} n_{ij}} = \sum_{j=1}^{m} v_j p(i, j), \tag{13}$$

where $A(a_{wi})$ is the annoyance rate of the i^{th} vibration intensity a_{wi}; n_{ij} is the number of subjective response of the j^{th} type of the i^{thi} vibration intensity; v_j is the membership value of the j^{th} type of unacceptable range, and $v_j = (j-1)/(m-1)$; m is the class number of the subjective response; if the classes of "no vibration feeling," "a little vibration feeling," "medium vibration feeling," "strong vibration feeling," and "extremely uncomfortable" are adopted to describe the subjective response of occupant, then $m = 5$; $p(i, j)$ represents the difference of the subjective feeling degree of the occupant:

$$p(i, j) = \frac{n_{ij}}{\sum_{j=1}^{m} n_{ij}}. \tag{14}$$

Considering the continuous distribution, calculation formula of annoyance rate is represented as

$$A(a_{wi}) = \int_{u_{\min}}^{\infty} \frac{1}{\sqrt{2\pi}\sigma_{\ln} u} \exp\left(\frac{-\left(\ln(u/a_w) + 0.5\sigma_{\ln}^2\right)^2}{2\sigma_{\ln}^2} \right) v(u) \mathrm{d}u, \tag{15}$$

where a_w is the frequency weighted vibration intensity; $\sigma_{\ln} = \sqrt{\ln(1 + \delta^2)}$, δ is the vibration coefficients and changes from 0.1 to 0.5, based on trial research, and $v(u)$ is the fuzzy membership function of vibration intensity, shown as follows:

$$\begin{cases} v(u) = 0, & u < u_{\min}, \\ v(u) = a \ln(u) + b, & u_{\min} < u < u_{\max}, \\ v(u) = 1, & u > u_{\max}, \end{cases} \tag{16}$$

where $u_{\min}$ is the top limit of "no feeling" to vibration of the occupant and $u_{\max}$ is the bottom limit of "extremely uncomfortable" to vibration of human being.

The coefficients of a, b can be obtained from the following equation:

Table 4: Calculation cases and results.

Case no.	Cross bridge interval (m)	Gantry rope diameter (mm)	Frequency weighted RMS acceleration aw (m/s^2)		Corresponding subjective response		Annoyance rate	
			Y	Z	y	z	Y	z
1	120	48	1.02	1.05			9.80%	11.87%
2	120	54	0.99	1.02			7.40%	9.66%
3	120	60	0.92	0.97	Uncomfortable		7.28%	7.72%
4	120	60	0.88	0.95			7.24%	7.70%
5	140	60	0.88	0.94			7.80%	8.13%
6	90	60	0.87	0.92	5.63%	5.58%		

$$\begin{cases} a \ln(u_{\min}) + b = 0, \\ a \ln(u_{\max}) + b = 1. \end{cases} \tag{17}$$

4.3. Parameter Study. As a temporary structure, old materials such as the gantry ropes from finished projects may be used to assemble the catwalk for the sake of economy. So there are many options for the catwalk rope sizes. However, the change in rope size will result the change of dynamic properties for catwalk, thus affecting the comfort level during construction. Cross bridge, which links two sides of the catwalk and increases the torsional stiffness of catwalk, is also an important part in the catwalk structure. The interval of cross bridges along the span (i.e., the number of the cross bridges) depends on the demand of engineering practice. A narrow cross bridge interval would waste materials and increase the construction cost, even though the safety of the catwalk is ensured adequately. However, wider cross bridge interval may cause smaller stiffness, affecting structural safety and decreasing comfort level due to vibration.

In that case, a set of rope size and cross bridge intervals listed in Table 4 are chosen to find out their influence on the vibration comfort. With each parameter change, buffeting analysis and comfort evaluation using two methods would be repeated. According to engineering practice, old materials are seldom used on the catwalk rope. The influence of catwalk rope size is neglected.

As previously stated, different cases were calculated and comfort level is listed in Table 4. From Table 4, we can find that these two methods of evaluating comfort yield consistent results. Compared with these results, the following conclusions can be summarized:

(1) The comfort evaluation method based on ISO 2631-1-1997 derives the consistent results with the annoyance rate method. The wind-induced vibration of the catwalk would cause the constructors to feel uncomfortable, while the least annoyance rate of 5.58% in the z-axis.

(2) The method based on ISO 2631-1-1997 can only evaluate the vibration comfort qualitatively, while the annoyance rate method can give a quantitative result.

(3) Enlarging the gantry rope size and narrowing the cross bridge interval would decrease the frequency weighted RMS acceleration and annoyance rate in both y- and z-axes.

(4) Enlarging the gantry rope size 12 mm in diameter decreases the annoyance rate by around 4%, while narrowing the cross bridge interval decreases the annoyance rate by 2.14% at most. So enlarging the gantry rope size is more efficient than decreasing the cross bridge interval.

5. Concluding Remarks

Based on the wind tunnel test and numerical analysis, the comfort level of the catwalk for Maputo Bridge was evaluated using qualitative and quantitative methods. The influences of structure parameters, like the size of gantry rope diameter and cross bridge interval, are investigated. Key conclusions can be summarized as follows:

(1) The traditional linear method will underestimate the buffeting response of the catwalk. The nonlinear method proposed in this paper can calculate the buffeting response of the catwalk more accurately. In the future, more catwalks with larger spans will be built, and the buffeting calculation should consider nonlinearity.

(2) The comfort evaluation method based on ISO 2631-1-1997 reaches the consistent results with the annoyance rate method. The former method can only evaluate the vibration comfort qualitatively, while the annoyance rate method can give a quantitative result.

(3) Enlarging the gantry rope size and narrowing the cross bridge interval would decrease the frequency weighted RMS acceleration and annoyance rate in both y- and z-axis. But enlarging the gantry rope diameter is more effective in boosting the comfort level.

This paper also suggests a framework to evaluate the comfort level due to wind-induced vibration based on annoyance rate model quantitatively. This method can also be extended to the assessment of vibration in other structures.

Data Availability

The mat data used to support the findings of this study are available from the corresponding author upon request.

Conflicts of Interest

The authors declare that they have no conflicts of interest to this work. The authors declare that they do not have any commercial or associative interest that represents a conflict of interest in connection with the work submitted.

Acknowledgments

This work was funded by National Natural Science Foundation of China (Grant no. 51778545), Science and Technology Projects of Power China (Grant no. SCMQ-201728-ZB), and Sichuan Provincial Science and Technology Program (Grant no. 2020YJ0310).

References

[1] H. Tanaka, "Aeroelastic stability of suspension bridges during erection," *Structural Engineering International*, vol. 8, no. 2, pp. 118–123, 1998.

[2] K. Kawaguchi and S. Fukunaga, "Structure of catwalk on the akashi kaikyo bridge," *Honshi Technical Representative*, vol. 19, no. 74, 1995.

[3] M. Takeno, H. Hosokawa, Y. Kishi, T. Okumoto, and T. Yoshioka, "Cable erection technology for world's longest suspension bridge-akashi kaikyo bridge," pp. 59–70, 1997, Nippon Steel Technical Report.

[4] M. Kitagawa, "Technology of the akashi kaikyo bridge," *Structural Control and Health Monitoring*, vol. 11, no. 2, pp. 75–90, 2004.

[5] S. Li, Y. An, and C. Wang, "Aerodynamic influence of the catwalks sectional dimension on steepled main cables in suspension bridges," in *Proceedings of the World Congress on Advances in Civil, Environmental, and Materials Research (ACEM16), the Structures Congress*, Jeju, Republic of Korea, April 2016.

[6] G. R. S. Assi and P. W. Bearman, "Transverse galloping of circular cylinders fitted with solid and slotted splitter plates," *Journal of Fluids and Structures*, vol. 54, pp. 263–280, 2015.

[7] S. Li and J. Ou, "Galloping analysis for the transient main cables of long-span suspension bridges during construction," *China Civil Engineering Journal*, vol. 42, no. 9, pp. 74–81, 2009.

[8] S. Zheng, H. Liao, and Y. Li, "Stability of suspension bridge catwalks under a wind load," *Wind and Structures*, vol. 10, no. 4, pp. 367–382, 2007.

[9] Y. Li, D. Wang, C. Wu, and X. Chen, "Aerostatic and buffeting response characteristics of catwalk in a long-span suspension bridge," *Wind and Structures*, vol. 19, no. 6, pp. 665–686, 2014.

[10] G. Wu, G. Fan, and J. Guo, "Ride comfort evaluation for road vehicle based on rigid-flexible coupling multibody dynamics," *Theoretical & Applied Mechanics Letters*, vol. 3, no. 1, Article ID 013004, 2013.

[11] W. W. Janssen, B. B. Blocken, and V. T. T. Hooff, "Computational evaluation of pedestrian wind comfort and wind safety around a high-rise building in an urban area," in *Proceedings of the 7th International Congress on Environmental Modelling and Software (iEMSs)*, San Diego, CA, USA, June 2014.

[12] P. Roy, "Maritime offshore operations-occupational noise monitoring, assessment and control," *The APPEA Journal*, vol. 49, no. 2, p. 569, 2009.

[13] C. Ma, J. Wang, Q. S. Li, and H. Liao, "3d aerodynamic admittances of streamlined box bridge decks," *Engineering Structures*, vol. 179, pp. 321–331, 2019.

[14] L. I. Sheng-li and O. U. Jin-ping, "Analysis of dynamic behavior of catwalks of long-span suspension bridge without windresistant cable," *Journal of Highway and Transportation Research and Development*, vol. 26, no. 4, pp. 47–53, 2009.

[15] G. Deodatis, "Simulation of ergodic multivariate stochastic processes," *Journal of Engineering Mechanics*, vol. 122, no. 8, pp. 778–787, 1996.

[16] R. H. Scanlan, "The action of flexible bridges under wind, I: flutter theory," *Journal of Sound and Vibration*, vol. 60, no. 2, pp. 187–199, 1978.

[17] ISO 2631-1, *Mechanical Vibration and Shock-Evaluation of Human Exposure to Whole-Body Vibration-Part 1: General Requirements*, International Organization for Standardization, Geneva, Switzerland, 1997.

[18] C. Tang, Y. Zhang, G. Zhao, and Y. Ma, "Annoyance rate evaluation method on ride comfort of vehicle suspension system," *Chinese Journal of Mechanical Engineering*, vol. 27, no. 2, pp. 296–303, 2014.

[19] Z. G. Song, *A New Annoyance-Based Vibration Comfort Design Theory on Engineering Structures*, Zhejiang University, Hangzhou, China, 2003.